applied microwave frequency is decreased from 17 to 7.5 GHz in 0.5 GHz steps. The distance between the pumping peaks, which is proportional to $2\Delta E$, decreases as the frequency is lowered. However, the peak distance decreases faster than linearly with frequency; the peaks follow the hyperbola rather than the straight lines. The distance goes to zero when the frequency approaches the minimum energy gap between bonding and antibonding states, $hf = 2T$. For frequencies smaller than the coupling, $hf < 2T$, the photon energy is too small to induce a transition from the bonding to the antibonding state.

The coupling between the dots can be decreased by changing the gate voltage on the centre gate to more negative values, or by applying a magnetic field perpendicular to the sample. In Fig. 4 we have plotted the frequency dependence of the energy spacing ΔE at which the pumping current is at a maximum. Different plotting symbols correspond to different centre gate voltage settings and magnetic fields. The solid lines are fits of equation (2) to the measured data. It follows that the coupling $2T$ has been tuned from 11 to 60 μeV. The good agreement with equation (2) and the clear nonlinear frequency dependence demonstrates the control over the formation of covalent bonding between the two dots.

Quantum dots have been suggested as possible candidates for building a quantum computer[14–16]. We have shown that it is indeed possible to coherently couple dots, and that one can induce transitions between the extended states. The next crucial step towards quantum logic gates is to show that the coherence of the superposition is preserved on timescales much longer than the time needed for manipulating the electron wavefunctions. A lower bound for the dephasing time is 1 ns, which we deduce from our narrowest peaks and from the smallest energy gaps between the bonding and antibonding states that we have resolved. We intend to perform measurements of the decoherence time in which the states are manipulated by applying the microwaves in short pulses. □

Received 15 April; accepted 15 July 1998.

1. Ashoori, R. Electrons in artificial atoms. *Nature* **379,** 413–419 (1996).
2. van der Vaart, N. C. *et al.* Resonant tunneling through two discrete energy states. *Phys. Rev. Lett.* **74,** 4702–4705 (1995).
3. Livermore, C. *et al.* The Coulomb blockade in coupled quantum dots. *Science* **274,** 1332–1335 (1996).
4. Blick, R. *et al.* Single electron tunneling through a double quantum dot: The artificial molecule. *Phys. Rev. B* **53,** 7899–7902 (1996).
5. Fujisawa, T. & Tarucha, S. Photon assisted tunneling in single and coupled quantum dot systems. *Superlatt. Microstruct.* **21,** 247–254 (1997).
6. Fujisawa, T. & Tarucha, S. Multiple photon assisted tunneling between two coupled quantum dots. *Jpn J. Appl. Phys.* **36,** 4000–4003 (1997).
7. Oosterkamp, T. H. *et al.* Photon sidebands of the ground state and first excited state of a quantum dot. *Phys. Rev. Lett.* **78,** 1536–1539 (1997).
8. Kouwenhoven, L. P. *et al.* in *Mesoscopic Electron Transport* (eds Sohn, L. *et al.*) 105–214 (NATO ASI Ser. E Vol. 345, 1997); also (http://vortex.tn.tudelft.nl/~leok/papers).
9. Leo, K. *et al.* Coherent oscillations of a wave packet in a semiconductor double-quantum well structure. *Phys. Rev. Lett.* **66,** 201–204 (1991).
10. Mendez, E. E. & Bastard, G. Wannier-Stark ladders and Bloch oscillations in superlattices. *Phys. Today* **46,** 34–42 (1993).
11. Flees, D. J. *et al.* Interband transitions and band gap measurements in Block transistors. *Phys. Rev. Lett.* **78,** 4817–4820 (1997).
12. Nakamura, Y. *et al.* Spectroscopy of energy-level splitting between two macroscopic quantum states of charge coherently superposed by Josephson coupling. *Phys. Rev. Lett.* **79,** 2328–2331 (1997).
13. Schedelbeck, G. *et al.* Coupled quantum dots fabricated by cleaved edge overgrowth: From artificial atoms to molecules. *Science* **278,** 1792–1795 (1997).
14. Landauer, R. Minimal energy requirements in communication. *Science* **272,** 1914–1918 (1996).
15. Barenco, A. *et al.* Conditional quantum dynamics and logic gates. *Phys. Rev. Lett.* **74,** 4083–4086 (1995).
16. Loss, D. & DiVincenzo, D. P. Quantum computation with quantum dots. *Phys. Rev. A* **57,** 120–126 (1998).
17. Stoof, T. H. & Nazarov, Yu. V. Time-dependent resonant tunneling via two discrete states. *Phys. Rev. B* **53,** 1050–1053 (1996).
18. Tien, P. K. & Gordon, J. R. Multiphoton process observed in the interaction of microwave fields with the tunneling between superconductor films. *Phys. Rev.* **129,** 647–651 (1963).
19. Stafford, C. A. & Wingreen, N. S. Resonant photon-assisted tunneling through a double quantum dot: An electron pump from spatial Rabi oscillations. *Phys. Rev. Lett.* **76,** 1916–1919 (1996).
20. Brune, Ph. *et al.* Photon-assisted transport through a double quantum dot with a time-dependent interdot barrier. *Physica E* **1,** 216–218 (1997).

Acknowledgements. We thank R. Aguado, S. M. Cronenwett, S. F. Godijn, P. Hadley, C. J. P. M. Harmans, K. K. Likharev, J. E. Mooij, Yu. V. Nazarov, R. M. Schouten, T. H. Stoof and N. C. van der Vaart for experimental help and discussions. This work was supported by the Dutch Organization for Research on Matter (FOM) and by the EU via the TMR network. L.P.K. was supported by the Dutch Royal Academy of Arts and Sciences (KNAW).

Correspondence and requests for materials should be addressed to T.H.O. (e-mail: tjerk@qt.tn.tudelft.nl).

Localized vibrational modes in metallic solids

V. Keppens*, D. Mandrus*, B. C. Sales*, B. C. Chakoumakos*, P. Dai*, R. Coldea*, M. B. Maple†, D. A. Gajewski†, E. J. Freeman† & S. Bennington‡

** Solid State Division, Oak Ridge National Laboratory, Oak Ridge, Tennessee 37831, USA*
† Department of Physics and Institute for Pure and Applied Physical Sciences, University of California San Diego, La Jolla, California 92093, USA
‡ ISIS Facility, Rutherford Appleton Laboratory, Chilton, Didcot, Oxfordshire, OX11 0QX, UK

Filled skutterudite antimonides[1,2] are cubic compounds with the formula RM_4Sb_{12}, where R is a rare-earth element (such as La or Ce), and M is a transition metal (for example, Fe or Co). The rare-earth ion is weakly bound in an oversized atomic cage formed by the other atoms. Its presence has been shown to cause a dramatic reduction in the lattice component of the thermal conductivity, while having little effect on the electronic properties[3–5] of the compound. This combination of properties makes filled skutterudites of interest as thermoelectric materials. It has been suggested[4] that localized, incoherent vibrations of the rare-earth ion are responsible for the reduction in thermal conductivity, but no direct evidence for these local vibrational modes exists. Here we report the observation of local modes in La-filled skutterudites, using heat capacity, elastic constant and inelastic neutron scattering measurements. The La atoms show unusual thermodynamic behaviour, characterized by the presence of two low-energy localized modes. Our results suggest that consideration of local modes will play an important role in the design of the next generation of thermoelectric materials.

Localized vibrational modes are uncommon in solids because of the strong interactions that exist between the constituent atoms. When present, local modes are usually associated with weakly bound guest atoms that reside in the voids of an open-structured non-metallic host. In metallic solids, which tend to crystallize in close-packed structures, local modes are exceedingly rare. These low-energy vibrational modes, which are not present in the unfilled parent compound $CoSb_3$, give unambiguous evidence for the 'rattling' behaviour of the rare-earth atom in the

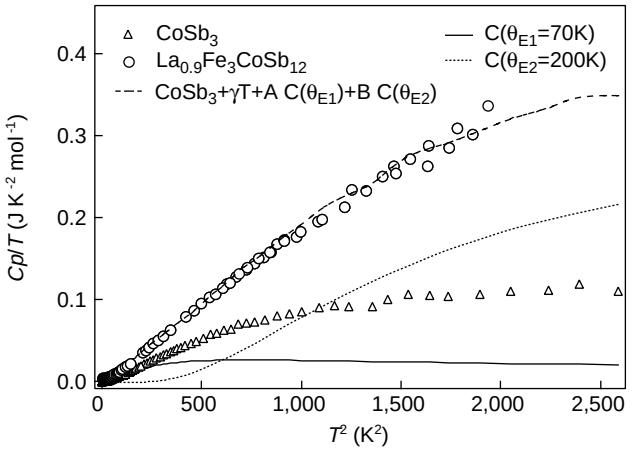

Figure 1 Specific heat divided by temperature versus temperature squared for $La_{0.9}Fe_3CoSb_{12}$ and $CoSb_3$. The dashed line through the $La_{0.9}Fe_3CoSb_{12}$ data is based on a calculation in which the contribution from two Einstein oscillators with level spacings of 70 and 200 K are added to the $CoSb_3$ data (see text for details).

structure. Because filled skutterudites display a wide variety of ground states, including metallic[3], semimetallic[6], semiconducting[4], superconducting[7], Kondo insulating[8] and ferromagnetic (both metallic[9] and insulating[8]), filled skutterudites offer a means to study the effects of localized atomic vibrations on a wide variety of physical phenomena.

Polycrystalline specimens were prepared by melting stoichiometric quantities of high-purity elements in carbon-coated, sealed and evacuated silica tubes. The details of the synthesis are described in ref. 4. Specific heat measurements were performed from 2 to 45 K for $CoSb_3$ and $La_{0.9}Fe_3CoSb_{12}$. The results are plotted in Fig. 1, which illustrates the significant difference in the low-temperature behaviour of the filled and unfilled materials. Although the specific heat of $CoSb_3$ deviates somewhat from simple Debye behaviour owing to the presence of some low-energy optical phonons involving collective motions of 4-membered Sb rings, a model proposed by Feldman and Singh[10] is able to quantitatively account for the data (J. Feldman, personal communication). Using the $CoSb_3$ data as a background, we find that the addition of two quantized harmonic oscillators (Einstein oscillators) is required in order to model the specific heat of $La_{0.9}Fe_3CoSb_3$. As illustrated in Fig. 1, a model calculation including the contribution of two Einstein oscillators leads to an adequate description of the experimental results. The dashed line through the $La_{0.9}Fe_3CoSb_{12}$ data in Fig. 1 represents a fit to the equation:

$$C_p = C_p(CoSb_3) + \gamma T + AC_{E1} + BC_{E2}$$

with $C_p(CoSb_3)$ the molar specific heat for $CoSb_3$, $\gamma = 0.0037\ mol^{-1}\ K^{-2}$, $A = 1.2\ mol^{-1}\ K^{-1}$, $B = 35.0\ mol^{-1}\ K^{-1}$ and T is temperature. Here C_{E1} and C_{E2} represent contributions from Einstein oscillators, $C_E = (\theta/T)^2 e^{(\theta/T)}/(e^{(\theta/T)} - 1)^2$, with Einstein temperatures $\theta_{E1} = 70$ K and $\theta_{E2} = 200$ K. The fact that two Einstein oscillators are required to model the data indicates that two distinct local modes may exist in the La-filled skutterudite. It is tempting to ascribe the lower-energy oscillator to the rattling of the La ions because the magnitude of the 70 K oscillator is about what we expect for a single ion oscillating in a harmonic potential. At high temperatures, we expect each mole of oscillators to contribute $3R = 24.95\ J\ K^{-1}$ to the heat capacity. As only ~5.3% of the atoms rattle, we anticipate a contribution of $\sim 1.33\ mol^{-1}\ K^{-1}$. This is very close to the fitted value of $1.21\ mol^{-1}\ K^{-1}$. We note that the results of the analysis are quite similar if one models the specific heat of $La_{0.9}Fe_3CoSb_{12}$ using a T^3 Debye term instead of the measured specific heat of $CoSb_3$. In that case two Einstein oscillators are again required, this time with $\theta_{E1} = 70$ K and $\theta_{E2} = 157$ K.

To investigate further the unusual thermodynamics of the La-filled skutterudite, we measured the elastic moduli of the filled and unfilled materials as a function of temperature. High-quality samples of $La_{0.75}Fe_3CoSb_{12}$, with a density that is 98% of the theoretical value, and $CoSb_3$ (95% dense) were cut into $2 \times 2.5 \times 3$ mm rectangular parallelepipeds and used for the resonant ultrasound spectroscopy (RUS) measurements. RUS is an unusual ultrasonic technique, developed by Migliori *et al.*[11] for determining the complete set of elastic moduli of a solid by measuring the free-body resonances of the sample. This method is unique in that all moduli can be determined simultaneously, avoiding remounts of transducers and multiple temperature sweeps. An isotropic polycrystalline solid has two elastic moduli, a shear modulus c_{44} governing transverse waves, and a compressional modulus c_{11} governing longitudinal waves. Measurements have been performed as a function of temperature (5–300 K) for both filled and unfilled skutterudite specimens. The upper panel of Fig. 2 shows the shear modulus c_{44} for $La_{0.75}Fe_3CoSb_{12}$, and in the inset the modulus for the unfilled skutterudite $CoSb_3$. The solid line through the $CoSb_3$ data is a model calculation, using the so-called Varshni function[12]:

$$c_{ij}(T) = c_{ij}^0 - s/(e^{t/T} - 1)$$

with T the temperature, c_{ij}^0 the elastic constant at 0 K, and s and t fitting parameters. This function was shown by Varshni to describe the temperature dependence of the elastic constants of many simple substances, and characterizes to some extent 'normal' elastic behaviour. The elastic response of $CoSb_3$ (Fig. 2) can be well-described by the Varshni model. However, the shear modulus of the filled skutterudite $La_{0.75}Fe_3CoSb_{12}$ behaves anomalously at low temperatures,

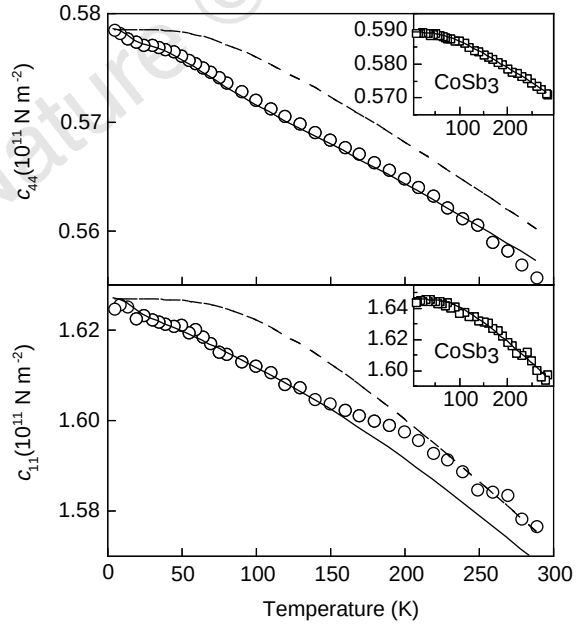

Figure 2 Elastic moduli c_{11} and c_{44} for $La_{0.75}Fe_3CoSb_{12}$ as a function of temperature. The solid lines through the data represent model calculations using two two-level systems; one with a level spacing of 50 K and the other with spacing of 200 K. The dashed lines are estimated background elastic moduli. The "normal" elastic behaviour of $CoSb_3$ is shown in the insets; the quantities plotted on the axes are the same as those in the main figures.

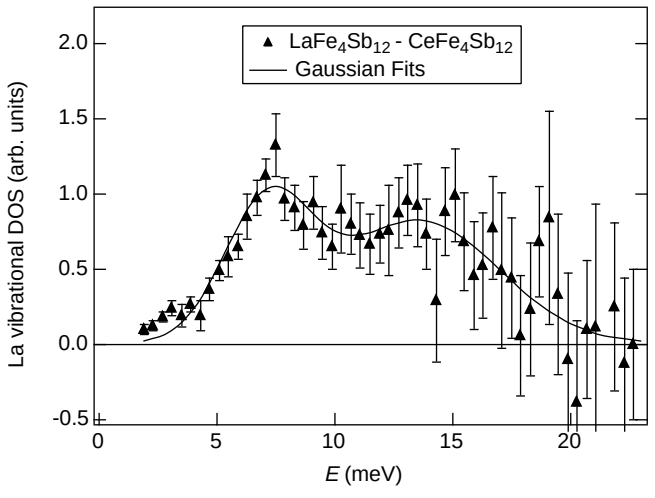

Figure 3 Difference in the inelastic neutron scattering data between $LaFe_4Sb_{12}$ and $CeFe_4Sb_{12}$ versus energy loss. The incident neutron energy was 30 meV and the energy resolution was ~2 meV. $CeFe_4Sb_{12}$ was used as a reference because the neutron scattering cross-section of Ce is much smaller than that of La. The difference spectra therefore reflect the vibrational density of states (DOS) associated with the La atoms. The peaks at 7 and 15 meV correspond to temperatures of 80 and 175 K.

displaying a much stronger temperature dependence, which is suggestive of unusual low-energy vibrational modes in addition to the normal acoustic phonons.

A first attempt to model this unusual behaviour, taking into account the presence of harmonic Einstein-oscillators, failed to describe the 'dip' in the data at low temperatures. The elastic data can, however, be described by considering the elastic response of a two-level system (TLS) with level-spacing Δ. We can calculate the TLS-contribution to the elastic response, $c = \partial^2 F/\partial\epsilon^2$, with $F = -N_A k_B T \ln(1 + e^{-\Delta/T})$ the Helmholtz free energy of a TLS, and assuming that the vibrational level spacing, Δ, depends linearly on the strain, ϵ, that is, $\Delta = \Delta_0 + A\epsilon$, with A a coupling constant. As illustrated in Fig. 2, both the c_{11} and c_{44} modulus can be modelled reasonably well by adding two TLSs, with level spacings of 50 and 200 K. The dashed line in Fig. 2 represents the 'background' contribution, which is estimated from the Varshni-fit for the unfilled skutterudite $CoSb_3$.

As the TLS approach quite effectively models the RUS data, whereas the Einstein modes fail, we investigated whether the specific heat, modelled above with two Einstein oscillators, could be described using two-level systems. We found that the data can indeed by modelled using two TLSs, with level spacing of 70 and 200 K. Both approaches seem to be indistinguishable in the experimental temperature range (2–45 K).

Inelastic neutron scattering can provide a quantitative measure of the vibrational density of states of a solid as a function of energy. Although quantitative interpretation of the data from a multi-element solid is only possible with a detailed model of the lattice dynamics, qualitative information can be extracted by comparing the measured vibrational spectrum to that of a suitable reference compound. Figure 3 shows the difference in the vibrational spectrum between $LaFe_4Sb_{12}$ and $CeFe_4Sb_{12}$ obtained from neutron-scattering measurements made at the ISIS facility of the Rutherford Appleton Laboratory, UK. The scattering cross-section for Ce is much less than for La, and hence this difference spectrum tends to emphasize the features of the vibrational spectrum associated with La. The neutron data show a well defined peak at 7 meV (80 K) and a somewhat broader feature at 15 meV (175 K). These energies are in good agreement with the values obtained from the heat capacity and RUS measurements. Truly localized modes should appear as delta functions in the vibrational density of states, but hybridization with acoustic phonons will tend to broaden the peaks.

The neutron data provide strong evidence that both local modes have to be associated with the presence of the La ion, suggesting that there are two distinct eigenmodes associated with the rattling of the ion. The structure of the material makes two different La motions likely. The rattling La ion can move towards one of its nearest neighbour Sb atoms, or it can move towards a 'void'. One would expect that if the La ion moves toward a 'void', its vibrations would have a lower frequency and be more localized than if it moved towards a nearest-neighbour Sb. The neutron results are consistent with this picture. The peak at 15 meV is considerably broader than the 7-meV peak, indicating that hybridization with other modes is stronger. This implies that the 15-meV mode is less localized than the 7-meV mode. Hybridization might also be the reason why Einstein oscillators cannot perfectly describe the local modes. Higher levels of the harmonic well that are hybridized with extended phonons will lose their 'local' character, effectively reducing the harmonic oscillator to a simple TLS.

To the best of our knowledge, the only metallic compound with a well-defined local phonon mode is $Al_{10}V$, which has[13] an Einstein temperature of 22 K. Compared to $Al_{10}V$, however, filled skutterudites have a number of advantages. Whereas $Al_{10}V$ poses formidable materials difficulties, filled skutterudites can be made single-phase and single crystals can be grown. Moreover, by controlling the filling of the rare-earth site, the carrier concentration and thus the transport properties of the material could be modified. Furthermore, various magnetic ions could be placed on the rare-earth site, and the effects of local phonon modes on a wide variety of ground states could be studied. □

Received 2 June; accepted 6 August 1998.

1. Jeitschko, W. & Braun, D. J. $LaFe_4P_{12}$ with filled $CoAs_3$-type structure and isotypic lanthanoid-transition metal polyphosphides. *Acta Crystallogr. B* **33,** 3401–3405 (1977).
2. Braun, D. J. & Jeitschko, W. Preparation and structural investigations of antimonides with the $LaFe_4P_{12}$ structure. *J. Less-Common Met.* **72,** 147–156 (1988).
3. Morelli, D. M. & Meisner, G. P. Low temperature properties of the filled skutterudite $CeFe_4Sb_{12}$. *J. Appl. Phys.* **77,** 3777–3781 (1995).
4. Sales, B. C. *et al.* Filled skutterudite antimonides: electron crystals and phonon glasses. *Phys. Rev. B* **56,** 15081–15089 (1997).
5. Sales, B. C., Mandrus, D. & Williams, R. K. Filled skutterudite antimonides: a new class of thermoelectric materials. *Science* **272,** 1325–1328 (1996).
6. Grandjean, F. *et al.* Some physical properties of $LaFe_4P_{12}$ type compounds. *J. Phys. Chem. Solids* **45,** 877–886 (1984).
7. Meisner, G. P. Superconductivity in $LaFe_4P_{12}$. *Physica B* **108,** 763–764 (1981).
8. Meisner, G. P. *et al.* UFe_4P_{12} and $CeFe_4P_{12}$: nonmetallic isotypes of superconducting $LaFe_4P_{12}$. *J. Appl. Phys.* **57,** 3073–3075 (1985).
9. Danebrock, M. E., Evers, C. B. H. & Jeitschko, W. Magnetic properties of alkaline earth and lanthanoid iron antimonides with the $LaFe_4P_{12}$ structure. *J. Phys. Chem. Solids* **57,** 381–387 (1996).
10. Feldman, J. L. & Singh, D. J. Lattice dynamics of skutterudites: first principles and model calculations for $CoSb_3$. *Phys. Rev. B* **53,** 6273–6282 (1996). Erratum **54,** 712 (1996).
11. Migliori, A. *et al.* Resonant ultrasound spectroscopic techniques for measurements of the elastic moduli of solids. *Physica B* **183,** 1–24 (1993).
12. Varshni, P. Temperature dependence of the elastic constants. *Phys. Rev. B* **2,** 3952–3958 (1970).
13. Caplin, D., Grüner, G. & Dunlop, J. B. $Al_{10}V$: An Einstein solid. *Phys. Rev. Lett.* **30,** 1138–1140 (1973).

Acknowledgements. We thank J. Feldman and R. Leisure for discussions, and A. Migliori and T. Darling for assistance with the RUS measurements. This work was supported by the Division of Materials Sciences, US Department of Energy, a Cooperative Research and Development Agreement with Marlow Industries, and the NSF.

Correspondence and requests for materials should be addressed to B.C.S. (e-mail: vb4@ornl.gov).

Synthesis of individual single-walled carbon nanotubes on patterned silicon wafers

Jing Kong*†, Hyongsok T. Soh†‡, Alan M. Cassell*, Calvin F. Quate‡ & Hongjie Dai*

* *Department of Chemistry,* ‡ *Department of Electrical Engineering, Stanford University, Stanford, California 94305, USA*
† *These authors contributed equally to this work*

Recent progress[1–3] in the synthesis of high-quality single-walled carbon nanotubes[4] (SWNTs) has enabled the measurement of their physical and materials properties[5–8]. The idea that nanotubes might be integrated with conventional microstructures to obtain new types of nanoscale devices, however, requires an ability to synthesize, isolate, manipulate and connect individual nanotubes. Here we describe a strategy for making high-quality individual SWNTs on silicon wafers patterned with micrometre-scale islands of catalytic material. We synthesize SWNTs by chemical vapour deposition of methane on the patterned substrates. Many of the synthesized nanotubes are perfect, individual SWNTs with diameters of 1–3 nm and lengths of up to tens of micrometres. The nanotubes are rooted in the islands, and are easily located, characterized and manipulated with the scanning electron microscope and atomic force microscope. Some of the SWNTs bridge two metallic islands, offering the prospect of using this approach to develop ultrafine electrical interconnects and other devices.

Our synthesis begins with the patterning of catalytic islands on silicon substrates. A schematic of the process flow is shown in Fig. 1. For regularly spaced catalytic islands on the silicon surface, the essential fabrication steps are: electron-beam lithography, deposition of $Fe(NO_3)_3{\cdot}9H_2O$, $MoO_2(acac)_2$ and alumina nanoparticles in the liquid phase and lift-off (Fig. 1). The square islands are spaced at a 10-μm pitch, and the size of islands is 3 μm or 5 μm. For